Mineralogical Magazine, August 1998, Vol. 62(4), pp. 477–486

Phenocrystic fluorite in peralkaline rhyolites, Olkaria, Kenya Rift Valley

A. S. MARSHALL

Environmental Science Division, Lancaster University, Lancaster LA1 4YQ, UK

R. W. HINTON

Department of Geology and Geophysics, Edinburgh University, Edinburgh EH9 3JW, UK

AND

R. MACDONALD

Environmental Science Division, Lancaster University, Lancaster LA1 4YQ, UK

ABSTRACT

The first occurrence of phenocrystic fluorite in a peralkaline rhyolite is reported from Quaternary lavas (agpaitic index 1.11–1.37) erupted from the Greater Olkaria Volcanic Complex, Kenya. Fluorite compositions are almost stoichiometric, with 0.65–1.49 ΣREE + Y oxides. Relative to coexisting glass (melt), the fluorites are enriched in *REE*, Y and Sr, are strongly depleted in all other trace elements and concentrate *MREE* relative to *LREE* and *HREE*. Y partitions into fluorite more strongly than the *HREE*. Fractionation of fluorite in its modal abundance would not significantly affect the *REE* abundances in the residual liquids, nor result in stronger Sr depletion. The *P*, *T* and composition conditions which stabilize fluorite in rhyolitic magmas are still obscure.

KEYWORDS: fluorite phenocrysts, peralkaline rhyolites, Kenya Rift Valley.

Introduction

ALTHOUGH fluorite occurs commonly as a late crystallizing mineral in granites, syenites, pegmatites and greisen, it has been recorded as a phenocryst phase only in topaz-bearing rhyolites from Utah (Christiansen *et al.*, 1983, 1986). Webster *et al.* (1987) recorded phenocryst clusters of biotite, fluorite, euxenite, thorite and zircon in vitrophyres from Spor Mountain, whereas Congdon and Nash (1988, 1991) described fluorite microphenocrysts in peraluminous, fluorine-rich pumices and vitrophyres of the Honeycomb Hills rhyolite. Fluorite has also been reported as a 'magmatic accessory' (Christiansen *et al.*, 1986) in many topaz rhyolites from Smelter Knolls, Utah, and from some topaz rhyolites in the Thomas Range and Wah Wah Mountains, Utah. In this paper we report a further occurrence of phenocrystic fluorite, the first from a peralkaline rhyolite. We also document the trace element partitioning between fluorite and coexisting melt (glass). Finally, we briefly examine the significance of the fluorite data for the *P*, *T* and volatile activity conditions under which the phenocrysts crystallized and for geochemical modelling of such rocks.

Geological setting

The Greater Olkaria Volcanic Complex (GOVC; Clarke *et al.*, 1990) is a multicentred Quaternary volcanic field near Lake Naivasha, within the inner trough of the Gregory Rift Valley in south-central Kenya (Fig. 1). At least 80 small volcanic centres, largely of mildly peralkaline rhyolite (comendite) composition have been identified. The earliest activity in the complex resulted in the growth of a trachyte-basalt lava and pumice pile, which was terminated at *c.* 20 ka by the formation

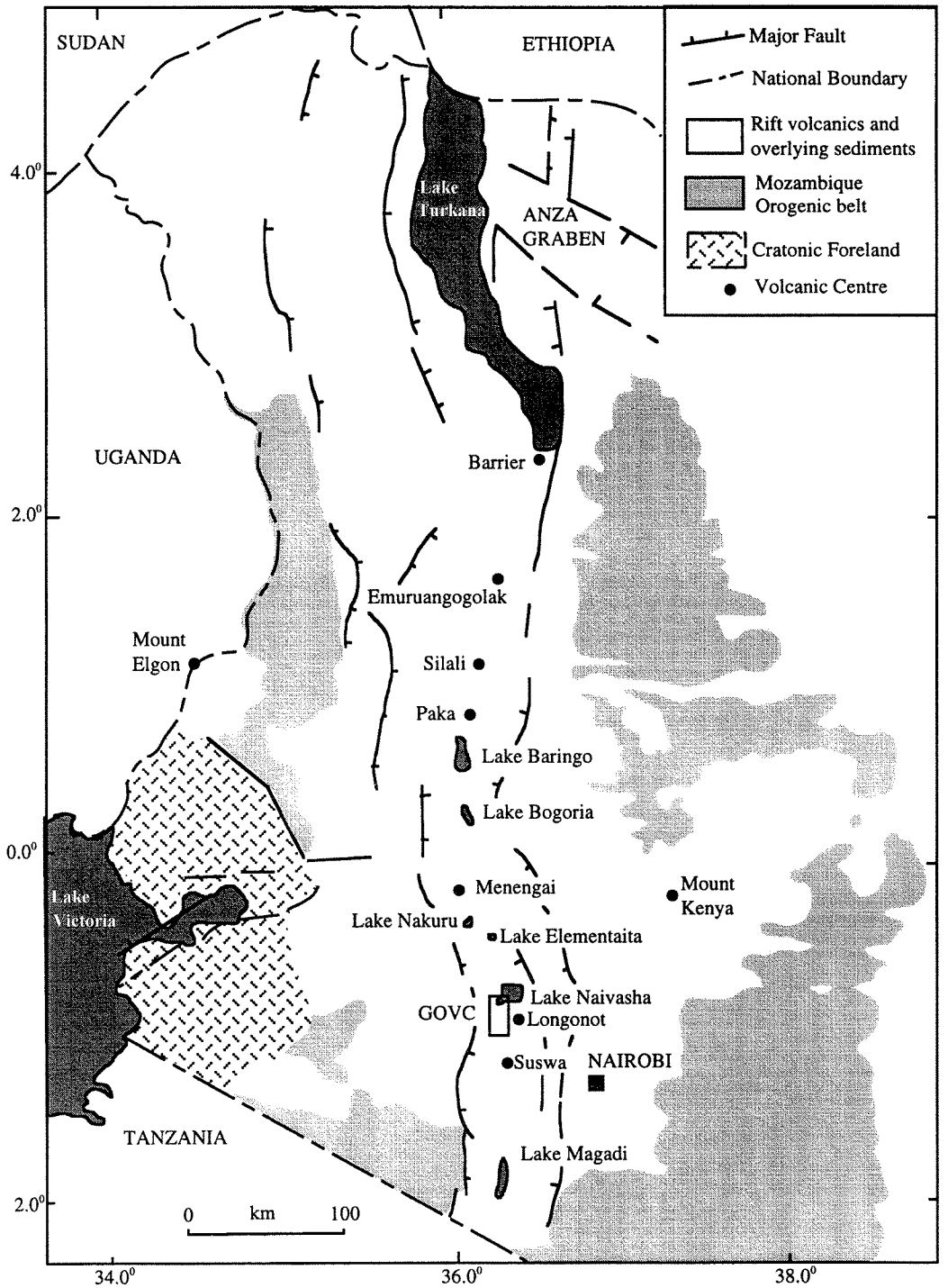

FIG. 1. Map of the Kenya Rift Valley. The Greater Olkaria Volcanic Complex (GOVC) is situated immediately south west of Lake Naivasha [modified from Black *et al.*, 1997].

of a caldera fracture associated with eruption of welded pantellerite ignimbrites (Clarke *et al.*, 1990).

The earliest post-caldera activity produced a series of lava domes and pyroclastic deposits (Lower Comendite Member of the Olkaria Comendite Formation; Clarke *et al.*, 1990). Following this phase of activity, an arcuate series of domes (Middle Comendite Member) were extruded along the caldera ring fracture. A period of resurgence then occurred during which superincumbent, short, thick, flows (Upper Comendite Member) were erupted. The most recent activity ($\geqslant$ 200 y B.P.) has been associated with the north-south trending Ololbutot fissure (Black *et al.*, 1997, Fig. 1*b*).

Chemical composition and phenocryst assemblages

The GOVC rhyolites range from mildly peralkaline (mol. $(Na_2O + K_2O)/ Al_2O_3 = 1.02$) to almost pantelleritic (1.40). The major element variations are typical of peralkaline rhyolites, specifically increases in Na_2O, FeO* and halogens, decreases in SiO_2, Al_2O_3, MgO and CaO, and constant K_2O, with increasing peralkalinity. The rocks also show trace element features characteristic of peralkaline compositions; for example high Nb, Ta, Zn, Zr, Hf and *REE*, and low Ba, Co, Sc and Sr abundances. The extreme enrichments and depletions of certain elements are striking, e.g. F (>1%), Nb ($\leqslant$ 1000 ppm), Zr ($\leqslant$ 4000 ppm), Sr (15 to $\leqslant$1 ppm) and Ba (50 to $\leqslant$1 ppm) (Clarke *et al.*, 1990; Black *et al.*, 1997).

Certain compositional features, such as linear correlations between incompatible trace elements, suggest that the GOVC rhyolites represent a single magmatic lineage. This, however, is too simple an interpretation. Macdonald *et al.* (1987) recognised seven, stratigraphically restricted groups on the basis of compositional differences. Current research by one of us (ASM) has extended the number of groups and revealed that there are sub-divisions within several of the groups of Macdonald *et al.* (1987), particularly in the Lower and Upper Comendite Members (Olenguruoni, Gorge Farm, Ololbutot centres; see Black *et al.*, 1997, Fig. 1*b*).

Phenocryst phases in the rhyolites are sanidine (Or_{40-46}), quartz, ferrohedenbergite, fayalite, titanomagnetite, ilmenite, biotite, riebeckite-arfvedsonite, aenigmatite, fluorite, chevkinite, apatite and zircon. Sanidine and quartz are ubiquitous; zircon occurs only in the least peralkaline rocks. Among the mafic phases, there is a tendency for ferrohedenbergite-fayalite-titanomagnetite assemblages to be replaced by riebeckite-arfvedsonite $\pm$ aenigmatite $\pm$ biotite assemblages as the rocks become more peralkaline. An example of coexisting titanomagnetite and ilmenite has yet to be recorded.

Analytical techniques

Major and trace element analyses of whole-rock samples were made using the Philips PW 1400 XRF facility at Lancaster University, using fused discs for major oxide determinations and pressed powders for trace element determinations. Glass and fluorite chemistries were determined using the Edinburgh University ion microprobe facility. Analyses were made with reference to NIST SRM 610 glass standard for glass and fluorite. Whilst the accuracy of the fluorite analyses has yet to be quantified (but is probably better than $\pm$ 15%), there is good correspondence between the XRF and ion microprobe glass analyses, particularly considering that one is whole rock and the other glass alone.

Mode of occurrence of fluorite

Fluorite phenocrysts have been found in lavas from 6 of the volcanic groups established by Marshall (in prep.) (Table 1). Table 2 contains whole rock data from three fluorite-phyric rhyolites; volcanic group names are from Marshall (in prep.), stratigraphic positions are from Clarke *et al.*, 1990. SMN87 (Arcuate Domes, O3, Middle Comendite Member), SMN61 (Olkaria, O4, Upper Comendite Member) and SMN49 (Gorge Farm, O4, Upper Comendite Member). All the analysed samples were pristine, non-hydrated glasses, as secondary hydration, crystallization and devitrification result in significant element mobility in peralkaline rhyolites (Noble, 1967; Rosholt *et al.*, 1971; Macdonald, 1974; Weaver *et al.*, 1990).

The lavas contain 1–16% total phenocrysts. Modal analyses of the three host rhyolites are presented in Table 3. Fluorite occurs as a colourless, often euhedral, hexagonal phenocryst phase up to 0.4 mm across. It occurs alone or showing mutual interfaces with sanidine (Fig. 2*a,b*), chevkinite, biotite and oxide phenocrysts. We see these interfaces as primary textural evidence that the fluorite is genuinely phyric.

TABLE 1. Phenocryst assemblages containing fluorite

Centre	Sample no.
Group 1	
S+Q+S/Q+Fa+Cpx+Ox+F	ND057
Olenguruoni	
S+Q+Cpx+F	OR337
Olkaria	
S+Q+(Z)+F	SMN61
S+Q+F	SMN133
Ololbutot	
S+Q+F	SMN40, 42–7
Arcuate Domes	
S+Q+S/Q+Il+Fa+Cv+F	SMN29
S+Q+S/Q+Ab+Il+Cv+F	SMN87
S+Q+Ox+F	OR542
Gorge Farm.	
S+Q+Ae(?)+Ox+F	SMN03
S+Q+Ab+Bi+F	SMN19
S+Q+S/Q+Ab+Ae(?)+Bi+F	SMN24
S+Q+S/Q+Ab+Ae(?)+Fa+Ox+F	SMN26
S+Q+Il+Bi+Cv+F	SMN49
S+Q+Ae(?)+Bi+F	SMN50,93
S+Q+Ab+Fa+TiMt+Bi+F	HG565
S+Q+S/Q+Ab+Fa+TiMt+Ae+F	HG570
S+Q+Bi+F	85–150

S = sanidine; Q = quartz; S/Q = sanidine-quartz intergrowths; TiMt = titanomagnetite; Il = ilmenite; Ox = Fe-Ti oxide; Cpx = ferrohedenbergite; Fa = fayalite; Ab = riebeckite-arfvedsonite; Bi = biotite; Ae = aenigmatite; Cv = chevkinite; Ap = apatite; Z = zircon; F = fluorite.
Brackets indicate microphenocryst

TABLE 2. Major and trace element analyses for three GOVC rhyolites

Sample no: wt %	SMN87	SMN61	SMN49
SiO_2	73.95	73.11	74.17
TiO_2	0.17	0.17	0.17
Al_2O_3	10.77	10.39	10.89
Fe_2O_3*	4.17	4.64	4.42
MnO	0.06	0.07	0.06
MgO	0.04	0	0
CaO	n.d.	n.d.	0.29
Na_2O	5.39	5.48	5.81
K_2O	4.40	4.19	4.34
Total	98.95	98.05	100.15
ppm			
Rb	501	535	741
Th	85	107	152
Pb	55	69	86
La	134	172	153
Ce	277	351	318
Zn	278	345	366
Nb	375	462	654
Y	214	259	330
Zr	1755	2249	2666

n.d. = not detected

Phenocrysts are occasionally twinned and may contain inclusions of chevkinite (Fig. 2*c*).

In comparison, lavas of the Honeycomb Hills, Utah, contain a greater percentage of phenocrysts (10–50%). Primary fluorite occurs as euhedral microphenocrysts (5–20 μm diameter) in vitrophyre and pumice. Fluorocerite [$(Ce,La)F_3$] forms colourless euhedral microphenocrysts (10–50 μm long) in vitrophyre or as inclusions (< 0.1 mm) in biotite phenocrysts in felsite (Congdon and Nash, 1988, 1991). Fluorite phenocrysts from Spor Mountain occur in clusters with biotite, euxenite, thorite and zircon, are euhedral and typically contain inclusions of biotite and accessory thorite, zircon and euxenite (Webster *et al.*, 1987).

Composition of fluorite

Compositional data for glass and fluorite phenocrysts in three rocks, obtained by ion microprobe, are presented in Table 4. The fluorites are close to CaF_2 in composition, in that the most abundant other components (the *REE* and Y) total between 0.65 and 1.49 (as oxides, wt.%). Figure 3 shows chondrite-normalised *REE* patterns for fluorite and glass; we believe that these are the first complete patterns published for fluorite phenocrysts. The fluorite patterns are similar for all three samples with slight enrichment from La to Sm, a strong, negative Eu anomaly, and decreasing abundances from Gd to Lu. The *LREE* part of the fluorite patterns is notably different to that in fluorocerite from Honeycomb Hill, Utah, where $[La/Sm]_N = 1.7$ (Congdon and Nash, 1991). In the GOVC fluorites there is modest *LREE* enrichment relative to *HREE*; $[La/Yb]_N$ values are in the range 2.87–3.45. The fluorite patterns differ in detail from those of

TABLE 3. Modal analyses of three GOVC rhyolites

	SMN87	SMN61	SMN49
Sanidine	3.16	2.33	3.15
Quartz	1.95	0.97	0.63
Sanidine/Quartz	1.95		
Ilmenite	0.45		0.11
Amphibole	1.05		
Biotite			0.21
Chevkinite	0.15		0.11
Fluorite	0.15	0.097	0.11
Glass	91.14	96.6	95.68

coexisting glass, where $[La]_N > [Sm]_N$ and $[Gd]_N \approx [Lu]_N$. However, Eu*/Eu matches very closely that of the coexisting glass (Fig. 3), Eu*/Eu = SMN87 0.15–0.14, SMN61 0.17–0.18, and SMN49, 0.10–0.10.

Fluorite–melt partition coefficients

Relative to the coexisting melts (glasses), the GOVC fluorites are enriched in *REE*, Y and Sr, and strongly depleted in all other analysed elements, ($K_D < 0.1$, except $K^{Cl}_{D\ fl/gl} = 0.212$ in SMN87; Table 5). $K^{REE}_{D\ fl/gl}$ are shown in Fig. 4. Values increase to a maximum at Gd and fluorite concentrates *MREE* relative to both *LREE* and *HREE*. Y partitions into fluorite more strongly than the *HREE*; $K^{Y}_{D\ fl/gl} = 13–25$.

$K^{Sr}_{D\ fl/gl}$ values of 50–77 indicate that fluorite concentrates Sr from magmas which are already Sr-depleted (typically 15 to $\leqslant 1$ ppm).

The unusual bell shaped pattern of fluorite-melt *REE* partitioning is similar to those for apatite and dacite melt (Nagasawa, 1970) and to those experimentally determined for apatites by Watson and Green (1981) who found that apatite/melt partitioning was composition dependent, $K^{Sm}_{D\ ap/melt}$ for example varying from ~4 in mafic melts to ~40 in water-rich granitic compositions. A major difference between the fluorite and apatite patterns is that Eu (as proxied by Sr in Watson and Green's study, 1981) partitioning into the apatites was low, resulting in a strongly negative Eu (Sr) anomaly in the partitioning patterns.

We can assess the significance of *REE* and Sr partitioning into the fluorite for modelling fractionation trends in peralkaline rhyolites. In SMN61 for example, fluorite phenocrysts with 451 ppm Gd (the most abundant *REE*) comprise 0.097% of the rock. Mass balance calculations indicate that < 2% of the rock's Gd budget is in fluorite. Fractionation of fluorite in its modal abundance would not significantly affect *REE* abundances in residual liquids.

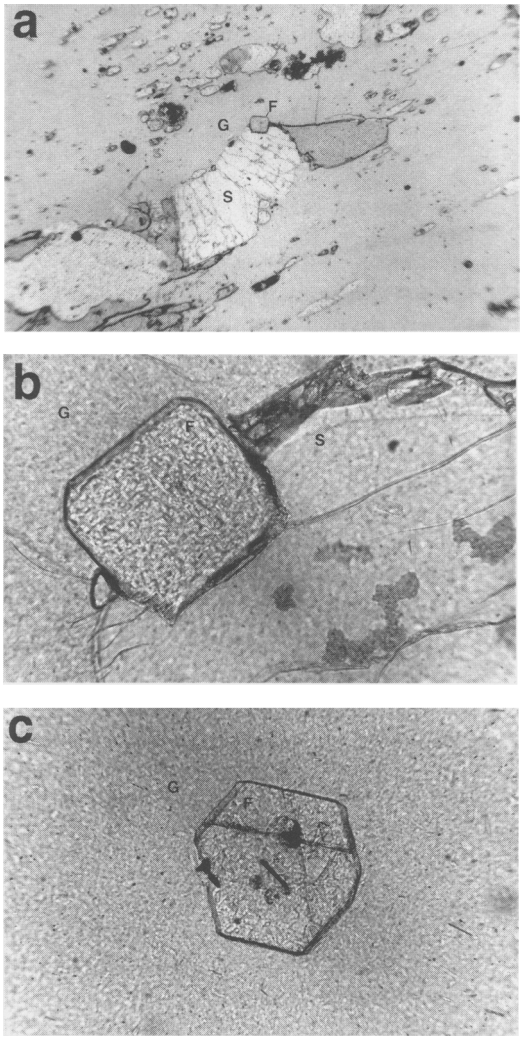

FIG. 2. Photomicrographs of fluorite phenocrysts. (*a*) Fluorite (F) showing mutual interfaces with sanidine (S) in glass (G) from SMN44 (Ololbutot, O4, Upper Comendite Member). PPL. Fluorite width 0.4 mm. (*b*) Detail of Fig. 2*a*, evidence of the phyric nature of fluorite (F). PPL. (*c*) Euhedral, hexagonal fluorite (F) with rod-shaped mineral inclusions of chevkinite, from SMN29 (Arcuate Domes, O3, Middle Comendite Member). PPL. Fluorite width 0.4 mm.

TABLE 4. Ion probe data for glass and fluorite phenocrysts (ppm) in the three GOVC rhyolites

Sample	Glass SMN87	Fluorite SMN87*	Glass SMN61	Fluorite SMN61	Glass SMN49	Fluorite SMN49
ppm						
Li	111	0.6±0.3	n.a.	n.a.	222	n.a.
Be	20.4	n.a.	n.a.	n.a.	n.a.	n.a.
B	19.5	n.a.	n.a.	n.a.	n.a.	n.a.
F	2143	n.a.	n.a.	n.a.	n.a.	n.a.
Na	53431	1262±101	n.a.	n.a.	n.a.	n.a.
Mg	59.0	12±1	n.a.	n.a.	84.6	n.a.
Al	49947	11±18	n.a.	n.a.	n.a.	n.a.
Si	345650	52.4±73.1	342000	3.51	348500	103
Cl	613	130±44	n.a.	n.a.	n.a.	n.a.
K	28677	20.5±28.2	n.a.	n.a.	n.a.	n.a.
Ca	448	n.a.	654	n.a.	240	n.a.
Ti	962	44.7	n.a.	n.a.	n.a.	n.a.
Mn	615	10.9±1.1	n.a.	n.a.	n.a.	n.a.
Fe	32878	20.1±24.5	n.a.	n.a.	n.a.	n.a.
Rb	301	n.a.	n.a.	n.a.	n.a.	n.a.
Sr	1.35	76±2.9	1.58	78.8	1.14	88.3
Y	199	2632±311	183	2970	226	5750
Zr	1720	n.a.	2090	n.a.	n.a.	n.a.
Nb	363	n.a.	442	0.533	593	0.409
Ba	3.03	0.126±0.1	2.76	0.470	2.41	0.155
La	119	245±37.8	136	353	63.0	593
Ce	243	634±89.8	276	960	194	1500
Pr	27.0	111±24	30.7	157	148	240
Nd	106	657±75	119	985	110	1420
Sm	22.4	227±23.9	26.4	323	69.1	493
Eu	0.504	6.5±1	0.792	10.3	0.459	9.49
Gd	24.8	327±41.7	28.6	451	30.1	782
Tb	4.99	45.5±9.6	6.33	74.4	6.92	123
Dy	32.8	271±62.2	41.5	397	45.9	678
Ho	6.97	48.9±6.9	7.87	71.6	9.34	123
Er	22.3	111±17.9	25.4	173	30.7	292
Tm	3.41	12.5±1.8	n.a.	17.2	n.a.	33.3
Yb	22.5	57.5±12.8	25.4	68.9	30.5	134
Lu	3.40	7.3±1.7	3.29	12.0	4.59	18.3
Th	n.a.	n.a.	54.4	0.814	76.6	0.411
U	n.a.	n.a.	14.1	0.675	18.9	0.045

* Mean of 4 analyses, S.D. 2σ. Ti, 1 analysis only.
n.a. = not analysed

The low modal abundance also means that even with a $K_{D\ fl/gl}^{Sr}$ of 50, only around 5% of the total Sr in SMN61 is in the fluorite. Fluorite crystallization alone would not result in Sr depletion in residual melts.

Conditions of fluorite crystallization

Christiansen *et al.* (1986) suggested that topaz rhyolites (± fluorite), of the western USA crystallized mostly at the lower end of the temperature range 850–600°C. f_{O_2} conditions appeared to have been variable, from ~ FMQ to NNO+3. High f_{HF} and f_{HF}/f_{H_2O} and probably high f_{HF}/f_{HCl}, were inferred from the composition of biotite phenocrysts.

The P–T–P_{vol} conditions under which the GOVC fluorite-phyric rhyolites crystallized are very poorly constrained, mainly as a result of the absence of suitable thermobarometers, such as

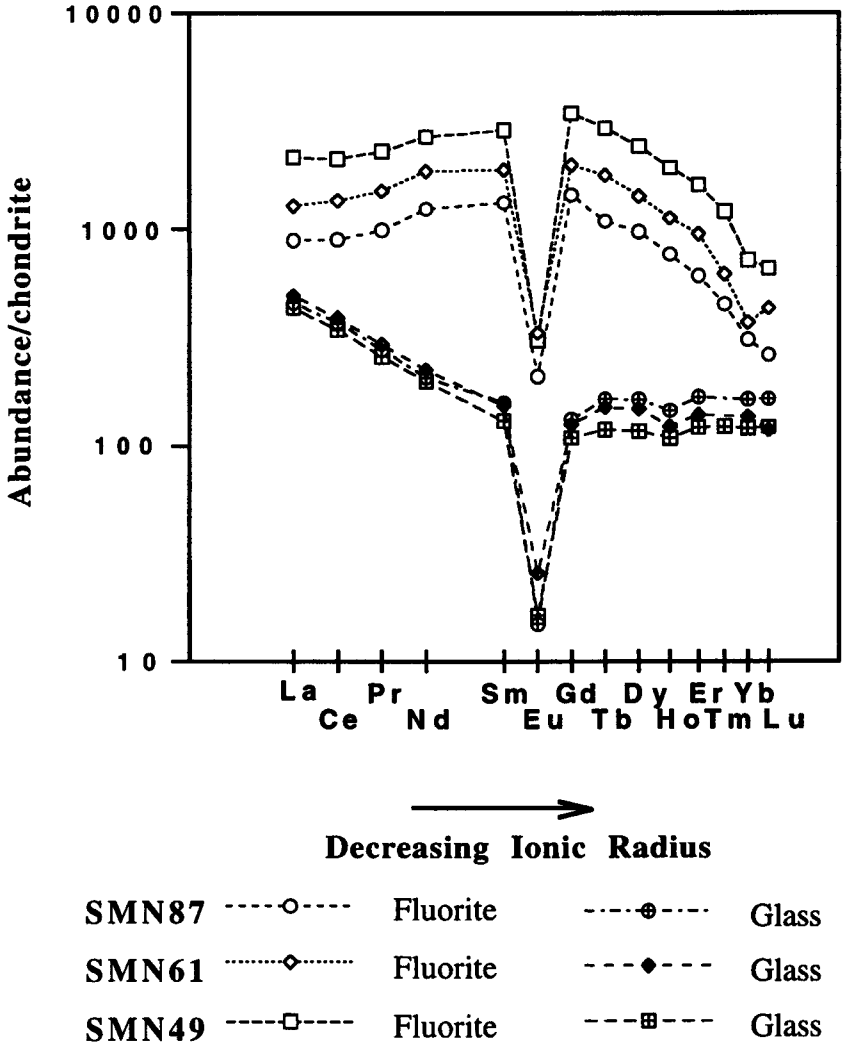

FIG. 3. Chondrite-normalised patterns for fluorite and glass from three GOVC rhyolites. Chondrite values from Anders and Grevesse (1989).

coexisting Fe-Ti oxides or pyroxenes. We can, however, briefly comment on possible compositional controls.

Fluorite crystallization at the GOVC is not simply related to melt peralkalinity or F concentration in the melt, since phenocrysts of fluorite are found in the least peralkaline (±Fa, ±Cpx) and most peralkaline (±Ae, ±Bi) assemblages, in rocks with agpaitic index ranging from 1.11 to 1.37 and F abundances from 0.2 to 1 wt.%. We cannot test quantitatively the possibility that the controlling factor was the H_2O/F ratio. Wilding *et al.* (1993) reported H_2O/F (wt) ratios between 0.23 and 20.9 in melt inclusions in quartz phenocrysts from 8 samples. The lower values certainly represent post-entrapment degassing but it is uncertain whether the higher values represent magmatic values or those after partial degassing.

In a study aimed mainly at greisen and porphyry deposits, Burt (1981) outlined qualitatively the stability of fluorite relative to other calcic phases, such as plagioclase, sphene (titanite) and clinopyroxene. Fluorite is apparently

TABLE 5. Partition coefficients for fluorite and coexisting glass in the three GOVC rhyolites

Element	SMN87 F/glass	SMN61 F/glass	SMN49 F/glass
Li	0.005	n.a.	n.a.
Na	0.024	n.a.	n.a.
Mg	0.031	n.a.	n.a.
Cl	0.212	n.a.	n.a.
Ti	0.046	n.a.	n.a.
Mn	0.018	n.a.	n.a.
Sr	56.3	49.9	77.5
Y	13.2	16.2	25.4
Nb	n.a.	0.001	0.001
Ba	0.042	0.17	0.064
La	2.05	2.6	4.78
Ce	2.61	3.48	5.81
Pr	3.82	5.11	8.25
Nd	6.22	8.28	12.9
Sm	10.1	12.2	18.1
Eu	12.9	13.0	20.7
Gd	13.2	15.8	26.0
Tb	9.12	11.8	17.8
Dy	8.26	9.57	14.8
Ho	7.02	9.1	13.12
Er	4.99	6.81	9.51
Yb	3.67	2.71	4.39
Lu	2.56	3.65	3.99
Th	n.a.	0.015	0.005
U	n.a.	0.048	0.002

n.a. = not analysed

stabilized in all cases by high μ_{HF}. Plagioclase and sphene are not present in GOVC rhyolites and we have found fluorite coexisting with clinopyroxene in two rocks where textural relationships do not allow us to judge whether or not they are in equilibrium.

Over the past 15 years there have been several experimental studies of the influence of fluorine on silicic melts. Increasing F concentrations affect the phase equilibria of feldspars and quartz (Manning, 1981; Luth and Muncill, 1989), lower melt viscosities (Dingwell *et al.*, 1985; Dingwell, 1988), increase the diffusivities of major elements through the melt (Dingwell, 1988) and affect the partitioning of ore producing elements between melt and fluid (Webster, 1990). Despite the high abundances of F in many of these experiments (up to 5 wt.%: Manning, 1981), fluorite has not been found as a near- liquidus phase; indeed, with one exception, it has not been recorded at all from the experimental crystalline assemblages. The exception is a glassy topaz rhyolite from Spor Mountain, Utah, which we noted earlier as containing fluorite in phenocryst clusters with biotite. The experimental work of Webster *et al.* (1987) indicated that the major phenocryst phases crystallized at pressures $\leqslant 1$ kbar and that the pre-eruptive water content was 5%. A small percentage of fluorite was found in run products near the solidus, 50–70°C below the biotite stability curve.

We have at this stage, therefore, little insight into the conditions under which the fluorite phenocrysts crystallized at Olkaria. Such information may best be gained by direct experimentation.

Acknowledgements

We thank Drs Peter Hill and Simon Burgess of the Edinburgh University Electron Microprobe Facility for their help and NERC Scientific Services for ion and electron probe support. Thanks for support also go out to Prof. Simon Harley at Edinburgh University. Lancaster work in Kenya is supported by the Natural Environment Research Council.

References

Anders, E. and Grevesse, N. (1989) Abundances of the elements: Meteoric and solar. *Geochim. Cosmochim. Acta*, **53**, 197–214.

Black, S., Macdonald, R. and Kelly, M.R. (1997) Crustal origin for peralkaline rhyolites from Kenya: Evidence from U-series disequilibria and Th-isotopes. *J. Petrol.*, **38**, 277–97.

Burt, D.M. (1981) Acidity–salinity diagrams — application to greisen and porphyry deposits. *Econ. Geol.*, **76**, 832–43.

Christiansen, E. H., Burt, D. M., Sheridan, M.F. and Wilson, R.T. (1983) The petrogenesis of topaz rhyolites from the western United States. *Contrib. Mineral. Petrol.*, **83**, 16–30.

Christiansen, E. H., Sheridan, M.F. and Burt, D.M. (1986) The geology and geochemistry of Cenozoic topaz rhyolites from the western United States. *Geological Society of America Special Paper*; **205**.

Clarke, M.C.G., Woodhall, D. G., Allen, D. and Darling, G. (1990) Geological, volcanological and hydrogeological controls on the occurrence of geothermal activity in the area surrounding Lake Naivasha, Kenya. *Nairobi: Ministry of Energy Report*, 1–60.

Congdon, R.A. and Nash, W.P. (1988) High-fluorine rhyolite: An eruptive pegmatite magma at the

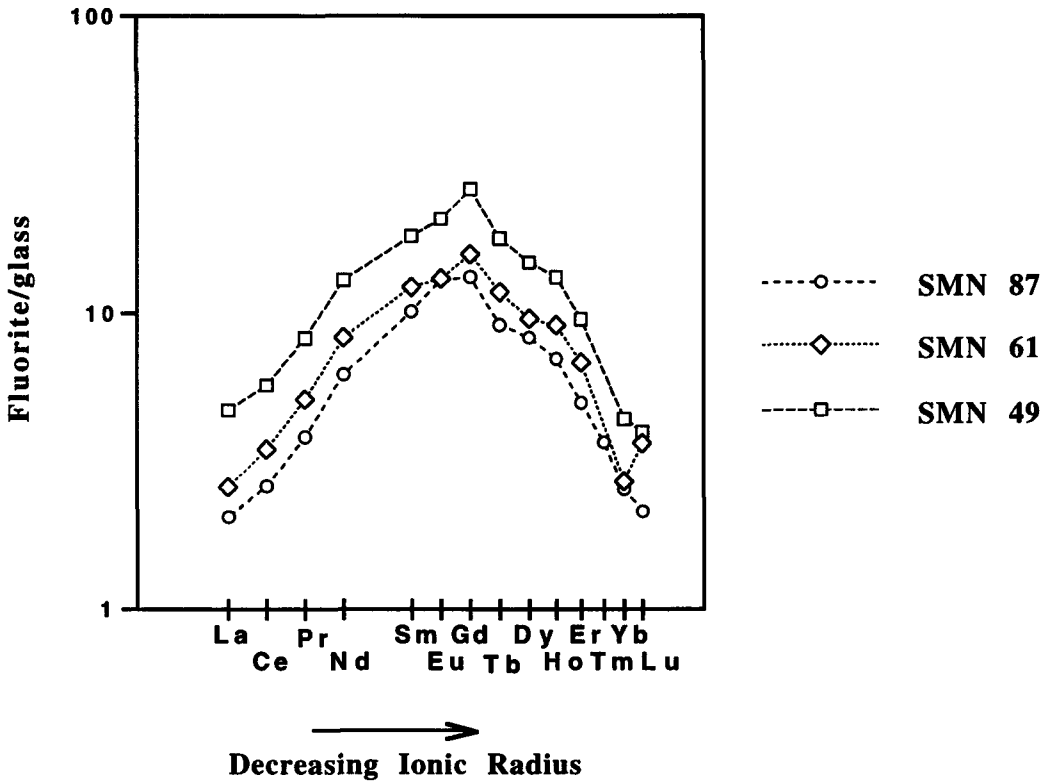

FIG. 4. *REE* partitioning between fluorite and glass.

Honeycomb Hills, Utah. *Geology*, **16**, 1018–21.

Congdon, R.A. and Nash, W.P. (1991) Eruptive pegmatite magma: Rhyolite of the Honeycomb Hills, Utah. *Amer. Mineral.*, **76**, 1261–78.

Dingwell, D.B. (1988) The structures and properties of fluorine-rich magmas: a review of experimental studies. *CIM Special Volume*, **39**, 1–12.

Dingwell, D.B., Scarfe, C.M. and Cronin, D.J. (1985) The effect of fluorine on viscosities in the system Na_2O–Al_2O_3–SiO_2: implications for phonolites, trachytes and rhyolites. *Amer. Mineral.*, **70**, 80–7.

Luth, R.W. and Muncill, G.E. (1989) Fluorine in aluminosilicate systems: Phase relations in the system $NaAlSi_3O_8$–$CaAl_2Si_2O_8$–F_2O. *Geochim. Cosmochim. Acta*, **53**, 1937–42.

Macdonald, R. (1974) Nomenclature and petrochemistry of the peralkaline oversaturated extrusive rocks. *Bull. Volcanol.* **38**, 498–516.

Macdonald, R., Davies, G.R., Bliss, C.M., Leat, P.T., Bailey, D.K. and Smith, R.L. (1987) Geochemistry of high-silica peralkaline rhyolites, Naivasha, Kenya Rift Valley. *J. Petrol.*, **28**, 979–1008.

Manning, D.A.C. (1981) The effect of fluorine on liquidus phase relationships in the system Qz–Ab–Or with excess water at 1 kb. *Contrib. Mineral. Petrol.*, **104**, 424–38.

Nagasawa, H. (1970) Rare earth concentrations in zircons and apatites and their host dacites and granites. *Earth Planet. Sci. Lett.*, **9**, 359–64.

Noble, D.C. (1967) Sodium, potassium, and ferrous iron contents of some secondarily hydrated natural silicic glasses. *Amer. Mineral.*, **52**, 280–86.

Rosholt, J.N., Prijana, S. and Noble, D.C. (1971) Mobility of uranium and thorium in glassy and crystallized silicic volcanic rocks. *Econ. Geol.*, **66**, 1061–9.

Watson, E.B. and Green, T.H. (1981) Apatite/liquid partition coefficients for the rare earth elements and strontium. *Earth Planet. Sci. Lett.*, **26**, 405–21.

Weaver, S.D., Gibson, I.L., Houghton, B.F. and Wilson, C.J.N. (1990) Mobility of rare earth and other elements during crystallization of peralkaline silicic lavas. *J. Volcan. Geotherm. Res.*, **43**, 57–70.

Webster, J.D. (1990) Partitioning of F between H_2O and CO_2 fluids and topaz rhyolite melt. *Contrib. Mineral. Petrol.*, **104**, 424–38.

Webster, J.D., Holloway, J.R. and Hervig, R.L. (1987) Phase equilibria of a Be, U and F-enriched vitrophyre from Spor Mountain, Utah. *Geochim. Cosmochim. Acta*, **51**, 389–402.

Wilding, M.C., Macdonald, R., Davies, J.E. and Fallick, A.E. (1993) Volatile characteristics of peralkaline rhyolites from Kenya: an ion microprobe, infrared spectroscopic and hydrogen isotope study. *Contrib. Mineral. Petrol.*, **114**, 262–75.

[*Manuscript received 18 August 1997: revised 23 December 1997*]